Reprinted with permission from: Korogiannaki M, Lyndon Jones L, Sheardown S. Impact of a Hyaluronic Acid-Grafted Layer on the Surface Properties of Model Silicone Hydrogel Contact Lenses. Langmuir 2019, 35, 950-961. DOI: 10.1021/acs.langmuir.8b01693 

# Impact of a Hyaluronic Acid-Grafted Layer on the Surface Properties of Model Silicone Hydrogel Contact Lenses

Myrto Korogiannaki,[†] Lyndon Jones,[‡] and Heather Sheardown*,[†]

[†]Department of Chemical Engineering, McMaster University, Hamilton L8S 4L8, Ontario, Canada

[‡]Centre for Ocular Research & Education, School of Optometry and Vision Science, University of Waterloo, Waterloo N2L 3G1, Ontario, Canada

**ABSTRACT:** The introduction of high oxygen transmissibility silicone hydrogel lenses ameliorated hypoxia-related complications, making them the most prescribed type of contact lens (CL). Despite the progress made over the last 2 decades to improve their clinical performance, symptoms of ocular dryness and discomfort and a variety of adverse clinical events are still reported. Consequently, the rate of CL wear discontinuation has not been appreciably diminished by their introduction. Aiming to improve the interfacial interactions of silicone hydrogel CLs with the ocular surface, a biomimetic layer of hydrophilic glycosaminoglycan hyaluronic acid (HA) (100 kDa) was covalently attached to the surface of model poly(2-hydroxyethyl methacrylate-co-3-methacryloxypropyl- tris-(trimethylsiloxy)silane) (pHEMA-co-TRIS) silicone hydrogel materials via UV-induced thiol-ene "click" chemistry. The surface structural changes after each modification step were studied by Fourier transform infrared spectroscopy–attenuated total reflectance and X-ray photoelectron spectroscopy (XPS). Successful grafting of a homogeneous HA layer to the surface of the model silicone hydrogels was confirmed by the consistent appearance of N (1s) and the significant decrease of the Si (2p) peaks, as determined by low-resolution angle-resolved XPS. The HA-grafted surfaces demonstrated reduced contact angles, dehydration rate, and nonspecific deposition of lysozyme and albumin, while maintaining their optical transparency (>90%). In vitro studies demonstrated that the HA-grafted pHEMA-co-TRIS materials did not show any toxicity to human corneal epithelial cells. These results suggest that surface immobilization of HA via thiol-ene "click" chemistry can be used as a promising surface treatment for silicone hydrogel CLs.

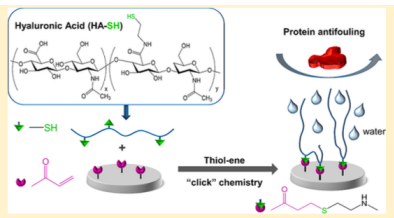

## INTRODUCTION

The contact lens (CL) industry was revolutionized by the development of silicone hydrogel (SiHy) lenses, which were first marketed in 1999. The introduction of silicone domains into the composition of soft CLs was a pivotal step in the development of CLs with superior oxygen permeability (Dk), while retaining the benefits of conventional hydrogel lens materials.[1,2] Consequently, SiHy CLs provide sufficient oxygen supply to the cornea to allow normal metabolic requirements to be met,[3] eliminating the hypoxia-related complications exhibited by earlier hydrogel-based CL materials, particularly when worn overnight.[4] However, because of the inherent hydrophobicity of silicone components, surface or bulk modification is necessary for SiHy lenses to avoid compromised surface properties such as decreased surface wettability, accentuated lens binding, and increased tear film-related biofouling,[5,6] which, in turn, lead to poor compatibility of the CL materials with the ocular environment.

Various techniques have been used for the improvement of surface wettability and hydrophilicity of SiHy lenses, including plasma surface treatments in the form of plasma coating or plasma oxidation[7,8] as well as the inclusion of a hydrophilic internal wetting agent.[9,10] More recently, SiHy materials based on either silicone-based macromers that impart naturally wettable surfaces that do not require further surface modification[11] or novel "water gradient" materials have been commercialized.[12] As evidenced by market trends, SiHy lenses are now the most widely prescribed soft CL category, accounting[13] for approximately 65% of new soft lens fits worldwide. Despite the different techniques developed to optimize the interactions between the SiHy lens and the ocular surface, resistance to protein and lipid deposition[14,15] and bacterial adhesion remains problematic, especially with over- night wear, potentially leading to sight-threatening microbial infections.[16] In addition, CL-induced dryness and discomfort, particularly at the end of the day, remain a major impediment to CL adoption.[17,18]

It is therefore clear that there remains considerable room for improvement in the performance of SiHy lenses. Although the factors that determine CL "biocompatibility" are numerous, complex, and interconnected, controlling the interactions of the eye–CL biointerface is of substantial importance.[19,20] To improve these interfacial interactions, SiHy-based materials have been typically coated or grafted with hydrophilic polymers, such as poly(ethylene glycol) (PEG) or poly- vinylpyrollidone.[21–23] Clinical data showed that the PEG surface-modified SiHy CLs reduced biofouling in vivo compared to unmodified commercial SiHy CLs.[21] Another approach was the development of zwitterionic surfaces based on the biomimetic polymer poly(2-methacryloyloxyethyl phosphorylcholine), a phosphorylcholine containing phospho- lipid polymer. These materials exhibited improved surface wettability, as well as highly repellent protein characteristics.[24] Taking advantage of the zwitterionic nature of hydrophilic natural amino acids, Xu et al.[25] developed serine-grafted SiHy materials that demonstrated good

hydrophilicity in vitro and better protein resistance than commercial SiHy CLs in vivo after a month of continuous wear.

Hyaluronic acid (HA) is a linear, anionic, nonsulfated glycosaminoglycan of the extracellular matrix naturally present in many tissues. In the eye, HA is found in the vitreous humor, in the lacrimal gland, as well as in the conjunctiva, corneal epithelium, and tear film.[26–29] Its ocular compatibility in combination with its unique viscoelastic, hygroscopic, shear- thinning, and lubricating properties renders HA well suited for ophthalmic applications, especially for the anterior ocular segment.[30] HA promotes tear film stability, ocular hydration, and effective lubrication.[31–33] It has been used effectively for the treatment of dry eye[34] and in CL products as a conditioning agent to alleviate dryness and discomfort during wear.[35]

The incorporation of HA into the bulk of model SiHy materials either as an internal or a releasable wetting agent or in the structure of an interpenetrating network led to enhanced wettable surfaces, which not only showed reduced nonspecific protein deposition[36–38] but also reduced lysozyme denaturation.[39] Surface immobilization of CLs with HA binding peptides was found to locally attract and concentrate exogenous HA, creating a thin HA coating that is able to retain moisture on the surface of the material.[40] Deposition of a self-assembled chitosan/HA multilayer coating, via electro- static interactions using the layer-by-layer technique, also improved surface characteristics such as wettability, dehy-dration, and resistance to protein sorption.[41] Finally, the bacteriostatic, antimicrobial, and antiviral properties of HA when used as a surface layer[42–44] further support its functionality as an efficacious surface layer for CL applications.

Thiol-ene “click” chemistry has been widely explored for biomaterial applications, including drug delivery, tissue engineering, and surface modification, owing to its rapid, cytocompatible, and bioorthogonal reactivity.[45,46] Thiol-ene chemistry can be catalyst mediated (Michael addition) or radical mediated (anti-Markovnikov radical addition). Radical-mediated thiol-ene reactions can be initiated either thermally or photochemically. Recently, photochemical routes have gained increased attention in the surface modification of polymeric materials for the development of controlled interfacial properties. Benefiting from the simplicity, robust nature, excellent chemoselectivity, and high reaction efficiency of “click” reactions, radical-mediated thiol-ene chemistry allows for reliable surface modification in a fast, modular fashion without compromising the bulk properties of the material.47 In addition, it can be performed under mild reaction conditions and it is tolerant to oxygen and water with minimal or no by- product formation, allowing for the modification of various types of surfaces, including that of living human cervical carcinoma cells (HeLa), without affecting their viability.[48] Further, it follows a step growth radical addition coupling mechanism that can be spatially and temporary controlled.[45] Photoinitiated thiol-ene reactions have been successfully established for photochemical surface modification processes, thus allowing for

applications in biomaterials, biomedicine, and biotechnology.[45,46] For instance, surface immobilization of HA on glass and silicon surfaces via UV-induced thiol-ene "click" chemistry resulted in more wettable surfaces with reduced protein deposition as well as cell adhesion and spreading characteristics.[49]

It has been recently demonstrated that covalent immobilization of HA on the surface of model poly(hydroxyethyl methacrylate) (pHEMA) hydrogels using thiol-acrylate "click" chemistry resulted in noncytotoxic materials with increased surface wettability, protein-resistant properties, and decreased dehydration rate.[50] This current study aims to investigate the impact that the surface-grafted HA has on the surface properties of model SiHy materials. Surface immobilization of HA was achieved by UV-initiated radical-mediated thiol-acrylate "click" chemistry, a versatile chemistry for the surface modification which enables efficient formation of the corresponding thioether bond with high specificity and fine control over the spatial arrangement of the surface chemical composition in synthetic processes.[51]

## EXPERIMENTAL SECTION

Materials and Chemical Reagents. HA (sodium hyaluronate) with an average molecular weight (MW) of 100 kDa was obtained from Lifecore Biomedical (Chaska, MN, USA). Hydroxybenzotriazole (HOBt) was purchased from Toronto Research Chemicals Inc (Toronto, ON, Canada). The monomer 3-methacryloxypropyl-tris- (trimethylsiloxy)silane (TRIS, ≥95%) was supplied by Gelest (Morrisville, PA, USA). In addition, the photoinitiators 1-hydroxy-cyclohexyl-phenyl-ketone (Irgacure 184) and 2-hydroxy-1-[4-(2- hydroxyethoxy)phenyl]-2-methyl-1-propanone (Irgacure 2959) were generously donated by BASF Chemical Company (Vandalia, IL, USA). The human corneal epithelial cell line (HCE-2 [50.B1] ATCC CRL-11135) was purchased from the American Type Culture Collection (Rockville, MD, USA). All other chemicals, reagents, and proteins were purchased from Sigma-Aldrich (Oakville, ON, Canada).

Synthesis and Characterization of Thiolated HA. For the synthesis of thiolated HA (HA-SH), the protocol followed was similar to that described previously.[50] Briefly, an aqueous solution of HA (100 kDa) (16.6 mg/mL, pH 7.4) was mixed with 3-(ethyl- iminomethyleneamino)-N,N-dimethylpropan-1-amine/HOBt (1:1 molar ratio) (3 equiv to –COOH of HA) at room temperature under stirring conditions for 1.5 h, while maintaining a pH of 6.8–7 (NaOH 1 M). Then, cysteamine dihydrochloride solution (3 equiv to –COOH of HA, 10 mL water) was added dropwise while the pH was kept stable at 7 (NaOH 1 M) (HA–SS–R) and the coupling reaction was allowed to proceed for 36 h at room temperature (pH 7, NaOH 0.1 M). The intermediate product HA–SS–R was exhaustively dialyzed against Milli-Q water using a dialysis membrane (MWCO 3.5 kDa, Spectra/Por, Spectrum Labs, CA). For the disulfide bond reduction, tris(2-carboxyethyl) phosphine hydrochloride HCl (35 mM, 5 equiv to –COOH of HA) was added in the HA–SS–R solution (pH 5, NaOH 1 M). After stirring for 7 h, the pH was reduced to 3.5 and the final solution was then purified by dialyzing (MWCO 3.5 kDa, Spectra/Por, Spectrum Labs, CA) in Milli-Q water (pH 3.5) for 5 days. The final product was freeze-dried and stored in the freezer (–20 °C) under nitrogen atmosphere to protect the free thiols from oxidation. The structure of the HA-SH product was determined by $^{1}$H NMR (20 mg/mL) using a Bruker

AVANCE 600 MHz (256 scans, room temperature) spectrometer using $D_2O$ as the solvent (D, 99.96%, Cambridge Isotope Laboratories, Inc.).

Ellman's Test Quantification of Free Thiols of HA-SH. The quantification of the free thiols of HA-SH was assessed spectrophoto- metrically, using Ellman's reagent (5,5′-dithiobis (2-nitrobenzoic acid)).[52] Briefly, unmodified HA and HA-SH were dissolved in sodium phosphate buffer (0.1 M, pH 8) containing 1 mM ethylenediaminetetraacetic acid. L-cysteine was used for the calibration curve (2–20 nmol, $R^2 = 0.9987$). After mixing the samples and L-cysteine standards with a solution of Ellman's reagent for 15 min at room temperature under dark conditions, the absorbance was measured at 412 nm using a UV–vis spectropho- tometer (SpectraMax Plus 384, Molecular Devices Corp.).

Synthesis of Model pHEMA-co-TRIS Hydrogel Materials. The monomers HEMA and TRIS, as well as the crosslinker ethylene glycol dimethacrylate (EGDMA), were passed through a polymer- ization inhibitor remover column prior to use. For the synthesis of the model pHEMA-co-TRIS hydrogels, HEMA and TRIS (90:10 wt %), as well as EGDMA (3.5 mol %), were mixed together vigorously for 30 min under a $N_2$ atmosphere. In turn, the photoinitiator Irgacure 184 (0.5 wt %) was added, and upon its dissolution, the prepolymer mixture was injected into a custom-made UV-transparent acrylic mold equipped with a 0.5 mm thick spacer. For the polymerization reaction, the prepolymer-containing mold was placed into a 400 W UV chamber ($\lambda = 365$ nm) (Cure Zone 2 CON-TROL-CURE, Chicago, IL, USA) for 10 min. Following an overnight post-curing period at room temperature, the model SiHy materials were taken out of the mold, placed into Milli-Q water to swell, and then punched into discs of 6.35 mm (1/4″) diameter. For extraction, the discs were soaked in a 1:1 (v/v) methanol/water solution for 12 h and subsequently in Milli-Q water for 24 h. Finally, the model SiHy discs were dried under ambient conditions and stored at room temperature.

Surface Acrylation of pHEMA-co-TRIS Hydrogel Materials. Initially, pHEMA-co-TRIS discs were dried overnight under vacuum. Taking advantage of the surface-active hydroxyl (–OH) groups of the HEMA domains, the introduction of α,β-unsaturated carbonyls on the surface of the model SiHy was achieved by the esterification reaction between the –OH groups and acryloyl chloride (Acr Cl). More specifically, the dried SiHy discs were immersed into an anhydrous dichloromethane (DCM) solution following dropwise addition of Acr Cl (29 mM per disc) and pyridine (Pyr) (0.1 equiv to Acr Cl used). The reaction proceeded for 3 h at room temperature and under $N_2$ and dark conditions. The surface-acrylated model SiHy discs (AcrpHEMA-co-TRIS) were then rinsed in dimethylformamide for 5 min (three changes) and washed in DCM and in Milli-Q water (three cycles each), with the washing procedure lasting for 24 h in total, to remove any unreacted chemicals as well as reaction by- products. Finally, the hydrogels were stored at room temperature in foil-covered glass vials containing Milli-Q water until further use.

Synthesis of Surface-Grafted HA-pHEMA-co-TRIS Hydrogel Materials. In a 20 mL glass vial, HA-SH (0.5 wt %) and the photoinitiator I2959 (0.1 wt %) were initially dissolved in Milli-Q-water. Into this solution, fully hydrated in Milli-Q-water AcrpHEMA- co-TRIS discs were submerged and the glass vial was immediately placed into a 400 W UV light chamber (Cure Zone 2 CON-TROL- CURE, Chicago, IL, USA), allowing for the surface-grafting thiol- acrylate

reaction to proceed at 365 nm for 10 min. At the end of the reaction, the surface-modified HA-pHEMA-co-TRIS discs were thoroughly washed for 24 h with Milli-Q-water to ensure that only grafted HA remained on the surface.

Surface Chemistry Characterization. Fourier Transform Infra- red Spectroscopy−Attenuated Total Reflectance. The surface chemistry of dry pHEMA discs after each surface modification step was analyzed using Fourier transform infrared spectroscopy− attenuated total reflectance (FTIR−ATR) (VERTEX 70 FTIR spectrometer, Bruker Instruments, Billerica, MA, USA) equipped with a diamond ATR cell. The absorption spectra used for the characterization were obtained at 64 scans with the resolution 4 $cm^{-1}$ ranging from 600 to 4000 $cm^{-1}$. A background spectrum was run and subtracted from the spectrum collected for each sample.

Angle-Resolved X-ray Photoelectron Spectroscopy. The chemical composition of the control and modified pHEMA-co-TRIS surfaces was determined by X-ray photoelectron spectroscopy (XPS). XPS measurements were performed using a PHI Quantera II XPS spectrometer (Physical Electronics (Phi), Chanhassen, MN, USA) equipped with a monochromatic Al Kα X-ray source (hv = 1486.7 eV). The X-ray anode was operated at 50 W and the high voltage was kept at 15 kV while the operating pressure of the analyzer chamber remained below $2.0 \times 10^{-8}$ Torr. The pass energy was fixed at 280 eV to ensure sufficient sensitivity, while a dual-beam charge compensation system was used for neutralization of all samples (beam diameter 200 μm), improving the energy resolution of the respective peaks.[53] Angle-resolved XPS (AR-XPS) was applied to obtain survey spectra at photoelectron take-off angles (defined as the angle between surface normal and the position of the analyzer) of 30°, 45°, and 90° for an in-depth analysis of the surface structure over a range of 3−10 nm.[54] All binding energies were referenced to the neutral C (1s) hydrocarbon peak at 284.8 eV. Survey scans were obtained in the 0−1350 eV range. Data manipulation of low-resolution spectra was performed using PHI MultiPak version 9.4.0.7 software. The survey spectra of three different spots per sample surface were collected to minimize error (n = 3 discs per sample).

Finally, the density (%) of the grafted HA layer on the surface of the pHEMA-co-TRIS hydrogels was calculated based on the following equation:

$$\text{Surface density (\%)} = 100 \times \frac{\frac{N}{C}}{\left(\frac{N}{C}\right)_{\text{theoretical}}} \qquad (1)$$

Contact Angle Measurements  Static Captive Bubble and Sessile Drop Techniques. The contact angle was measured using the captive bubble as well as the sessile drop technique (optical contact angle analyzer  OCA 35, DataPhysics, Germany). Initially, the surface of fully swollen discs was blotted with a Kimwipe to remove free water. For the captive bubble technique, the disc was initially immersed into a chamber filled with Milli-Q water and a 5 μL air bubble was placed on the surface of the disc. The Milli-Q water in the chamber was replaced prior to measuring the contact angle of each set of samples. For the sessile drop technique, a 5 μL drop of Milli-Q water was placed on the surface of the disc. In both techniques, the drop was allowed to settle on the surface and the contact angle between the bubble/drop and the hydrogel surface was

calculated with a video-based software (SCA 20, DataPhysics Instruments, Germany). To account for potential inhomogeneities on the surface of the samples, the contact angle of two different spots from both sides of each disc was measured (n = 6 discs per sample). All measurements were made at ambient humidity and temperature.

Dehydration Kinetics and Equilibrium Water Content. The impact of surface grafting of HA on the dehydration rate of the pHEMA-co-TRIS samples was determined by measuring the mass change over time. Briefly, the samples equilibrated in Milli-Q water were gently blotted with a Kimwipe to remove excess water and placed in a closed chamber digital balance with an incorporated digital hygrometer (La Crosse Technology, WT-137U, RH = 32 ± 2% at 24 °C) using a custom-made holder which allows for exposure of both surfaces of the discs for evaporation. The samples were weighed immediately after placement ($W_{wet}$, t = 0) as well as at different time intervals ($W_t$, t = 1–150 min). Finally, the discs were dried overnight in a 50 °C oven and reweighed ($W_{dry}$).

The water loss (%) used to express the dehydration rate was calculated based on the following equation:

$$\text{Water loss}\ (\%) = \frac{W_{wet} - W_t}{W_{wet} - W_{dry}} \times 100\% \qquad (2)$$

The equilibrium water content (EWC) of the model SiHy was also calculated:

$$\text{EWC}\ (\%) = \frac{W_{wet} - W_{dry}}{W_{wet}} \times 100\% \qquad (3)$$

**Scheme 1. Schematic Illustration of the Synthesis of Thiolated-HA (HA-SH)**

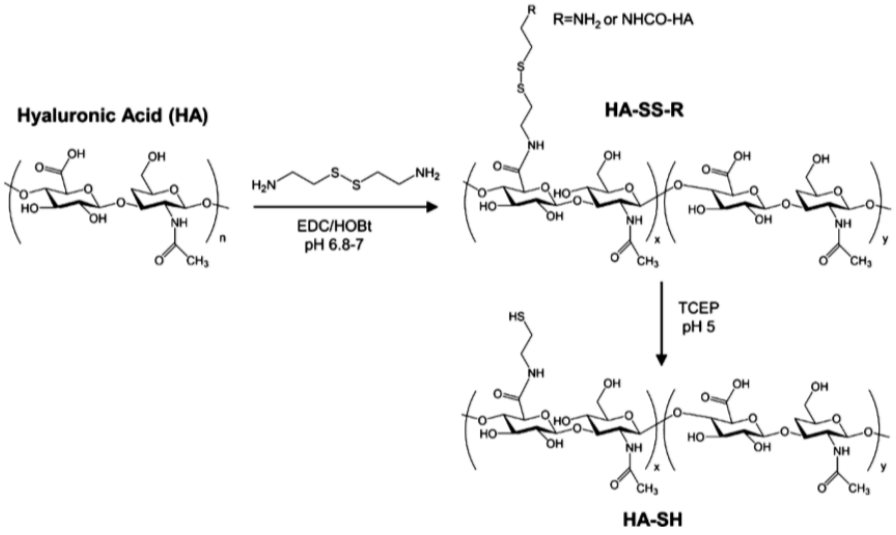


Optical Transparency. The optical properties of the model SiHy materials after each modification

step were assessed by measuring the transmittance (%) of fully hydrated pHEMA-co-TRIS SiHy discs immersed into 100 μL of Milli-Q water for the range of 400–750 nm, using a UV–vis spectrophotometer (SpectraMax Plus 384, Molecular Devices, Corp, Sunnyvale, CA, USA).

In Vitro Protein Deposition  Lysozyme and Human Serum Albumin. For the quantification of the nonspecifically adhered lysozyme (from chicken egg white) and human serum albumin (HSA) on the surface of the pHEMA-co-TRIS surfaces, proteins were radiolabeled with $I^{125}Na$ using the iodine monochloride method.[55] After the iodination reaction, unbound $I^{125}$ was removed by passing the labeled protein through a column packed with AG 1-X4 (Bio-Rad, Hercules, CA, USA). The percentage of free iodide, which was determined by the trichloroacetic acid precipitation assay, was found to be less than 0.5% of the total activity for both labeled protein solutions. A single-protein solution (1 mg/mL) of each protein of interest was prepared in phosphate-buffered saline (PBS) (pH 7.4) containing 5 wt % of the radiolabeled $I^{125}$–protein.

The pHEMA-co-TRIS discs, equilibrated in PBS (pH 7.4), were individually incubated into each single-protein solution (250 μL/disc) for 6 h at room temperature. The samples were then washed three times with fresh PBS (pH 7.4) (5 min intervals) to remove loosely adherent proteins. Each disc was then blotted dry with a Kimwipe, placed in a counting vial (5 mL nonpyrogenic, polypropylene round- bottom tube), and counted for radioactivity using a Gamma Counter (PerkinElmer Wallac Wizard 1470 Automatic Gamma Counter, Wellesley, MA, USA). The radioactivity associated with the surfaces was converted into a protein amount using a standard calibration curve. The results are presented as the mass of protein sorbed per disc surface area (n = 6 discs per sample).

In Vitro Cell Viability. The cytocompatibility of the pHEMA-co- TRIS model SiHy after each modification step was determined using immortalized human corneal epithelial cells (HCECs) and the 3-(4,5- dimethylthiazol-2-yl)-2,5-diphenyltetrazolium bromide (MTT) assay. This colorimetric assay is based on the reduction of yellow tetrazolium salt MTT to water-insoluble dark blue formazan salt by metabolically active cells. Briefly, immortalized HCECs (HCE-2 [50.B1] ATCCR CRL-11135TM from the American Type Culture Collection, Rockville, MD) were suspended in culture medium ($1.5 \times 10^5$ cells/mL) and seeded in a flat-bottom 96-well culture plate (100 μL culture medium per well). The culture medium included a keratinocyte serum-free medium (KSFM) supplemented with human recombinant epidermal growth factor 1-53 (EGF 1-53) and bovine pituitary extract. After incubating the HCECs in a humidified 5% $CO_2$ environment at 37 °C for 24 h to ensure adhesion, the culture medium was removed and replaced with fresh KSFM (250 μL). The swollen pHEMA-co-TRIS SiHy that previously were extensively washed with sterile PBS (pH 7.4) for 6 h at room temperature were then inserted in the HCEC-containing wells vertically and away from the bottom of the well. The positive control of this study was cultured cells without pHEMA-co-TRIS discs. At the end of a 24 h incubation period in a cell culture incubator (5% $CO_2$, 37 °C), the discs were discarded and the media were aspirated while each well was gently rinsed with PBS pH 7.4. For the assay, 10 μL of the MTT solution (5 mg/mL in PBS pH 7.4) and 100 μL of PBS were added in each well, and the plate was then covered with foil and placed in the cell incubator for 4 h. Subsequently, 85 μL of the above solution was removed, while the resulting formazan salt was dissolved in 50 μL of dimethyl sulfoxide. The absorbance of the solubilized formazan product was measured at 540 nm

using a UV–vis spectrophotometer (SpectraMax Plus 384, Molecular Devices, Corp, Sunnyvale, CA, USA), with the absorbance value being proportional to the number of viable cells remaining following the incubation period. The reported cell viability (%) was expressed by the ratio of absorbance of the cells in the presence of the SiHy discs to that of the cells incubated with culture medium only (positive control). For cell viability values lower than 70%, the materials were considered potentially cytotoxic.[56]

Statistical Analysis. Data are presented as mean ± standard deviation (SD). Statistical analysis was determined/performed by a single-factor analysis of variance with post hoc Tukey's honestly significant difference test in Statistica 10.0 StatSoft Inc., Tulsa, OK, USA). A p value $<0.05$ was considered to be statistically significant.

## RESULTS AND DISCUSSION

Synthesis and Characterization of HA-SH. The functionalization of HA with thiol groups included a condensation and a reduction reaction, as previously described by Korogiannaki et al.[50] (Scheme 1). Taking advantage of the carboxyl group (–COOH) in the HA backbone, the amidation reaction between HA and cystamine dihydrochloride was accomplished by a carbodiimide-mediated reaction resulting in the formation of the intermediate HA–SS–R. Commercially available TCEP was chosen for the subsequent reduction reaction (HA-SH) instead of the commonly used 1,4- dithiothreitol because it is a faster and stronger reducing agent.[57] The yield of this two-step reaction was approximately 90%.

The structure of the final thiomer HA-SH was confirmed by $^1$H NMR in $D_2O$. In Figure 1, the resonance at 2.03 ppm ($\delta_a$) was attributed to the acetamide moiety of the N-acetyl-D- glucosamine residue (–NHC(O)$CH_3$) group and the peaks from 3.3 to 4 ppm correspond to the methine groups on the six-membered rings of HA backbone, respectively (Figure 1A). Compared to the $^1$H NMR spectrum of the native HA, the new signals centered at 2.93 and 2.72 ppm were assigned to the methylene protons ($CH_2CH_2SH$) ($\delta_{b+c}$) of the cysteamine moieties (Figure 1B), indicating the successful modification of HA with thiol functional groups (HA-SH). Finally, the free- thiol content of HA-SH, quantified by Ellman's method, was 793.1 ± 34.3 nmol SH/mg HA, which in turn corresponds approximately to 32 ± 1.3 free thiols per 100 repeat/ disaccharide units of HA. No free thiols were detected in the native HA and in the intermediate HA–SS–R product. This moderate degree of HA thiolation is not expected to affect its hydrophilic anionic character, bioactivity, and toxicity while providing adequate anchoring sites with the surface of interest for the modification of the model SiHy materials.

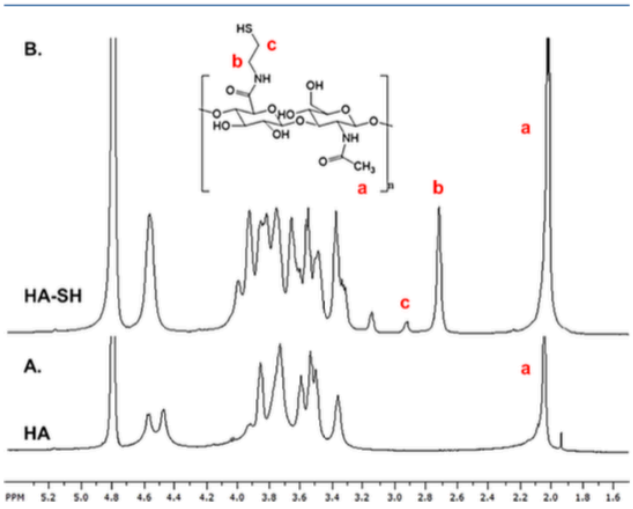


**Figure 1.** Characteristic $^{1}$H NMR spectrum (600 MHz) of (A) unmodified HA (100 kDa) and (B) HA-SH.

Synthesis and Surface Chemistry Characterization of the HA-Grafted pHEMA-co-TRIS (HA-pHEMA-co-TRIS) Hydrogel Materials. Surface immobilization of HA on the model SiHy substrate was achieved by free-radical thiol-ene "click" chemistry. Scheme 2 depicts the procedure followed for the preparation of the HA-pHEMA-co-TRIS materials. The coupling reaction of HA-SH with the acrylate groups present on the pHEMA-co-TRIS surface was photochemically induced in the presence of Irgacure 2959 (I2959) which is water soluble and widely used in thiol-acrylate reactions, without causing any cellular toxicity.[58] Upon exposure to 365 nm UV light, I2959 undergoes homolytic bond cleavage resulting in the formation of thiyl radicals (RS$^{\bullet}$). The direct addition of the thiyl radical across the C C double bond of the acrylate group yields an intermediate β-thioether carbon-centered radical, which in turn is able to abstract a hydrogel from another thiol moiety resulting in the formation of a new thiyl radical as well as the final hydrothiolation product that exhibits anti-Markovnikov orientation (Scheme 2). This type of reaction generally exhibits step growth radical addition mechanism, with the propagation and chain-transfer steps occurring consecutively, ensuring quantitative formation of the desired thioether in a modular fashion.[59] In thiol-acrylate chemistry, apart from the hydrothiolation reaction, there is a chance of homopolymerization of the acrylate groups upon UV exposure,[45] leading to a combination of step and chain growth mechanisms. This homopolymerization reaction, however, is considered to be minimal in the present work because of steric hindrance of the surface acrylate groups. The limiting step of the surface modification reaction is therefore considered to be the chain-transfer step of the thiol-acrylate grafting reaction.[60] The organic solvent (DCM) was selected for the intermediate acrylation reaction because it did not cause a change of mass for the pHEMA-co-TRIS hydrogels. In addition, the

grafting reaction occurred in fully swollen samples and under ambient atmosphere, as thiol-ene photoreactions have been reported to be relatively unaffected by oxygen.[45] Overall, the facile and relative fast surface modification process chosen herein is based on already commercially available materials that are not expensive, allowing for a scalable and thus commercially relevant method for the formation of a HA-grafted layer to the surface of the model SiHy materials.

The model SiHy used in this research are based on a hydrophilic (HEMA) and a hydrophobic siloxane-based (TRIS) monomers as well as a crosslinker (EGDMA) widely used in the commercial CL materials. However, commercial SiHy lenses contain different ratios of the hydrophobic/ hydrophilic phase and/or more components which are not included here because of patent and industrial restrictions. Moreover, the shape and the dimensions of the model SiHy materials used herein (flat discs) differ from those of the commercial CLs. Therefore, any comparison of the examined characteristics below between the developed HA-grafted model SiHy materials and commercial SiHy CLs would not lead to accurate conclusions.

**Scheme 2. Schematic Illustration of Grafting HA to pHEMA-*co*-TRIS Surface via UV-Induced Free-Radical Thiol-Ene "Click" Chemistry; (A) Pristine pHEMA-*co*-TRIS, (B) Acrylated pHEMA-*co*-TRIS (AcrpHEMA-*co*-TRIS), and (C) HA-Grafted pHEMA-*co*-TRIS (HA-pHEMA-*co*-TRIS) Surfaces**

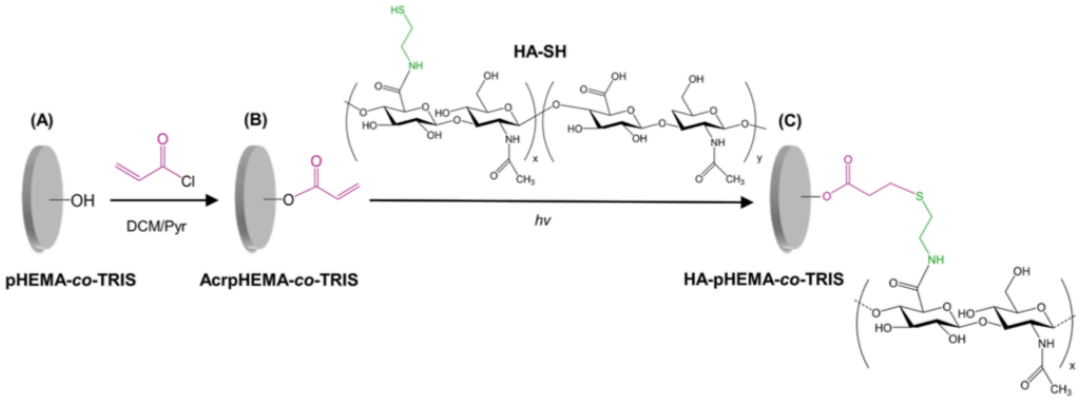


Surface Chemistry Characterization of HA-SH Grafted to AcrpHEMA-co-TRIS (FTIR–ATR and XPS). The chem- istry of the model SiHy surfaces before and after each modification step was determined by FTIR–ATR and XPS (Figures 2 and 3). All ATR–FTIR measurements were performed on dehydrated samples in order to avoid the impact of bound water on the spectra. Upon reaction of the pHEMA-co-TRIS with the Acr Cl, a decrease in the broad absorbance band at approximately 3405 $cm^{-1}$ of the –OH stretching vibration in combination of the presence of a new absorption band at 1635 $cm^{-1}$, which was assigned to the bending vibrations of C C bonds, suggested successful surface acrylation of pHEMA-co-TRIS surfaces (Figure 2B). This procedure introduced

α,β-unsaturated carbonyls to the surface of the model SiHy allowing for further reaction with the –SH groups of HA (HA-pHEMA-co-TRIS). For the HA- modified samples, however, the surface sensitivity of FTIR– ATR was not adequate to detect the expected modifications associated with the covalent attachment of HA on their surface (Figure 2C), as the sampling depth of FTIR–ATR is a few hundred nanometers, whereas the surface-grafted HA layer is expected to have a thickness of several tens of nanometers. Hence, XPS was used to confirm the surface conjugation reaction.

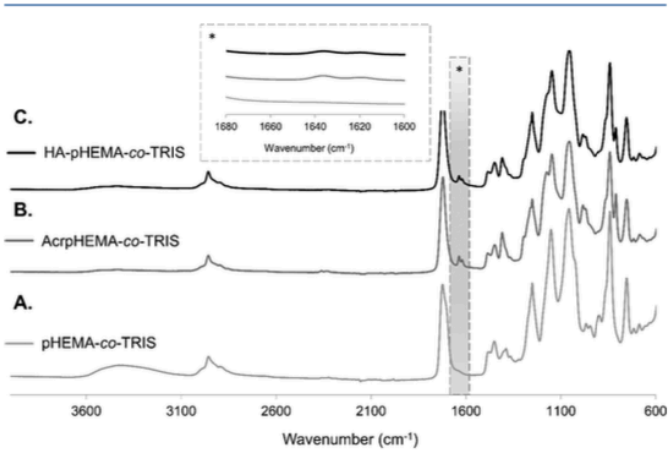


**Figure 2.** FTIR–ATR spectra from (A) pristine pHEMA-*co*-TRIS, (B) AcrpHEMA-*co*-TRIS, and (C) HA-pHEMA-*co*-TRIS surfaces.

Because of its exceptional surface sensitivity, XPS analyses were performed to gain more insight into the chemical functionalization of the outermost (10 nm) surface layer of the model SiHy surfaces, with up to 0.1% sensitivity.[54] A typical XPS survey spectrum of the unmodified, acrylated, and HA- grafted pHEMA-co-TRIS surfaces at 45° take-off angles is depicted in Figure 3. As anticipated, the distinct peaks observed for the pristine and acrylated pHEMA-co-TRIS surfaces (Figure 3A,B) at 530 and 283 eV as well as 151 and 100 eV were assigned to oxygen ($O_{1s}$), carbon ($C_{1s}$), and silicon ($Si_{2s}$ and $Si_{2p}$) respectively. The presence of the new peak at approximately 397 eV in the HA-pHEMA-co-TRIS surface spectrum was attributed to the nitrogen ($N_{1s}$) (Figure 3C), indicating that the HA had been successfully grafted to the surface of the model SiHy by UV-induced thiol-acrylate chemistry. The presence of the chemical bond between the HA layer and the SiHy substrate is expected to retain the durability of the modified surfaces even after the autoclaving process, which is traditionally used for the sterilization of CL materials.

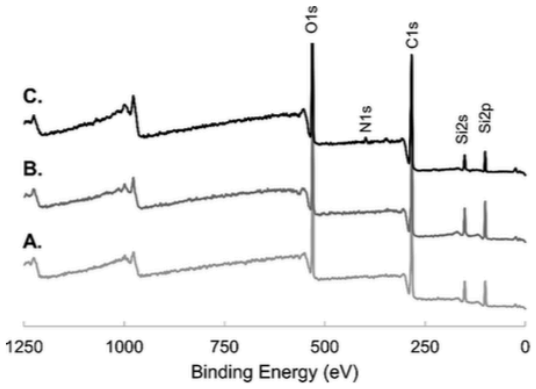


**Figure 3.** Representative XPS survey spectrum at 45° take-off angle for dehydrated (A) pristine pHEMA-*co*-TRIS, (B) AcrpHEMA-*co*-TRIS, and (C) HA-pHEMA-*co*-TRIS surfaces.

In addition, the presence of concentration gradients in the near-surface region was qualitatively evaluated by AR-XPS. Table 1 shows the composition of the surfaces at different take- off angles. Apart from the presence of the $N_{1s}$ signal, the O/C ratio of the HA-pHEMA-co-TRIS surfaces was significantly higher for all three take-off angles compared to those of the pristine and the intermediate surface-acrylated SiHy ($p < 0.001$), in a similar manner to that previously observed for HA- linked surfaces.[61,62] AR-XPS is an effective tool for non- destructive depth profile analysis of the elemental composition of the near-surface regions of the model SiHy materials (usually from 3 to 10 nm of the outermost surface) by manipulating the photoelectron angle of take-off with respect to the surface normal.[63] Accordingly, by decreasing the take-off angle, the penetration depth from which the photoelectrons are accepted is shallower, therefore enhancing the surface sensitivity of the XPS analysis.[64] AR-XPS, unlike AFM or sputtering methods, can also provide a nondestructive measurement of the thickness of a thin surface film or the thickness of an overlayer.[64]

**Table 1. Surface Elemental Compositions (%) of the HA-Grafted Silicone Hydrogels Determined by AR-XPS Measurements at Three Different Take-Off Angles (30°, 45°, and 90°)**

| material | angle (deg) | $C_{1s}$ | $N_{1s}$ | $O_{1s}$ | $Si_{2p}$ | O/C | Si/C |
|---|---|---|---|---|---|---|---|
| control | 30 | 67.1 ± 1.6 | | 21.9 ± 1.0 | 11.0± 1.1 | 0.33 ± 0.02 | 0.16 ± 0.02 |
| acrylated | | 66.0 ± 4.7 | | 21.9 ± 2.6 | 12.1 ± 2.3 | 0.34 ± 0.06 | 0.19 ± 0.05 |
| HA grafted | | 64.7 ± 1.6 | 1.7 ± 0.2 | 28.0 ± 1.0 | 5.7 ± 1.0 | 0.43 ± 0.02 | 0.09 ± 0.02 |
| control | 45 | 66.7 ± 2.4 | | 23.0 ± 1.9 | 10.2 ± 0.6 | 0.35 ± 0.04 | 0.15 ± 0.01 |
| acrylated | | 69.5 ± 2.9 | | 20.3 ± 2.3 | 10.2 ± 1.7 | 0.29 ± 0.04 | 0.15 ± 0.03 |
| HA grafted | | 65.1 ± 1.4 | 2.0 ± 0.6 | 27.3 ± 1.2 | 5.7 ± 0.7 | 0.42 ± 0.03 | 0.09 ± 0.01 |
| control | 90 | 66.3 ± 3.0 | | 24.0 ± 2.0 | 9.6 ± 1.8 | 0.36 ± 0.04 | 0.15 ± 0.03 |
| acrylated | | 65.2 ± 2.1 | | 24.7 ± 1.3 | 9.8 ± 1.4 | 0.37 ± 0.03 | 0.14 ± 0.03 |
| HA grafted | | 65.2 ± 1.2 | 1.1 ± 0.3 | 28.9 ± 1.1 | 4.5 ± 0.9 | 0.45 ± 0.02 | 0.07 ± 0.01 |

Moreover, the Si signal of HA-pHEMA-co-TRIS was significantly decreased ($p < 0.0001$), even in the case of the 90° take-off angle, which represents an approximate 10

nm depth of penetration, further confirming the presence of a thick graft layer of HA able to effectively mask the underlying substrate, which in turn limited the silicon detection even in the high-vacuum environment of the XPS. Similar or even higher Si content was also detected at the outermost surface region of commercial surface-treated SiHy CLs (balafilcon A and lotrafilcon A).[53,65] This is thought to be the result of the

high flexibility and mobility of the silicone–oxygen chains, often resulting in their migration to the outer interface, even if they have to overcome a surface layer of a hydrophilic polymer.[66,67] The O/C as well as the Si/C ratio of the model SiHy surfaces remained almost the same when the take-off angle was increased, suggesting that the samples were characterized by a consistent and homogeneous chemical composition throughout their near-surface region.

Finally, the density (%) of HA on the surface of the developed silicone hydrogels for the 30°, 45°, and 90° take-off angles was determined. As the degree of thiolation of HA (100 kDa) used for the surface grafting reaction is 32 ± 1.3%, the theoretical values of $N_{1s}$ and $C_{1s}$ are approximately 54.3 and 4.8% per chain. In this case, the theoretical N/C ratio is 0.089, assuming 100% coverage of HA on the surface of the silicone hydrogel material. On the basis of eq 1, the density (%) of HA on the surface of the developed pHEMA-co-TRIS hydrogels for the 30°, 45°, and 90° take-off angles is 29 ± 4.2, 34 ± 5, and 19 ± 4.5 respectively, while an average value from all angles is approximately 28%. It is important to note that calculating the surface density from AR-XPS would be an estimate at best, given that the surface HA layer is dehydrated and under high vacuum during the experiment. In hydrated state, surface- grafted HA is expected to cover more space as it can absorb water up to 1000 times its weight in water and thus increase its surface volume.

Surface Wettability. Surface wettability is a particularly relevant property for CLs as it is associated with tear film spreading and stability upon insertion.[68] In this study, the surface wettability of the model SiHy was evaluated in vitro as a function of the contact angle measured by the sessile drop and the captive bubble techniques. According to Maldonado- Codina et al.,[68] the sessile drop can be used to measure advancing contact angle, which can be indicative of the ease with which the eyelids can reform the tear film (initial tear film spreading) over a fully or partially dehydrated lens surface, while the captive bubble technique is presumably an indication of the tear film stability on the fully hydrated lens surface during the blinking cycles. Hence, these two techniques are considered of equal importance for a good estimation of the in vivo wetting properties of the model SiHy surfaces, even though they measure two different types of contact angle. For both techniques, decrease in the measured contact angle implies improved surface wettability.

As shown in Figure 4, substitution of the surface hydroxyl groups with the α,β-unsaturated carbonyls slightly increased the contact angle of the AcrpHEMA-co-TRIS (p

< 0.04) for both sessile drop and captive bubble techniques. The HA- pHEMA-co-TRIS sample, however, exhibited significantly reduced contact angles (sessile drop: 60%, $p < 0.0002$ and captive bubble: 40%, $p < 0.002$), suggesting improved surface wettability. This observation can also be used as another indication of the successful covalent attachment of HA on the surface of the model SiHy. Improved surface wettability is of great importance for SiHy CLs, as their inherently hydro- phobic silicone components can migrate to the surface and cause poor in vivo wettability, leading to visual disturbances, increased lens surface deposition, and ocular dryness.[69,70] In addition, the surface wettability was not found to be affected over time as the contact angle of the developed materials remained stable in the course of 3 weeks (data not shown). Of note, a 4-fold increase in the concentration of either HA-SH or the initiator I2959 did not cause any further decrease in the contact angle (sessile drop) (data not shown), suggesting that the concentration of HA-SH (0.5 wt %) and I2959 (0.1 wt %) resulted in the maximum grafting density under the conditions examined. Interestingly, increasing the I2959 concentration to above 0.1 wt % led to cause gelation of the HA-SH solution, even in the presence of TCEP (pH 5) and under $N_2$ conditions. To the best of our knowledge, this has not been reported before in the research literature. Lower concen- trations for either HA-SH or I2959 were not examined.

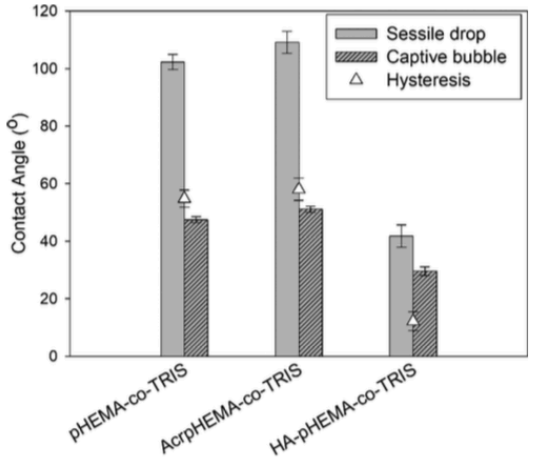


**Figure 4.** Static water contact angle (±SD) of pristine pHEMA-*co*-TRIS, AcrpHEMA-*co*-TRIS, and HA-pHEMA-*co*-TRIS hydrogels ($n$ = 6) using sessile drop and captive bubble techniques. The hysteresis, defined as the difference between the contact angle of the sessile drop and that of the captive bubble techniques, as a function of surface treatment is also depicted.

Finally, the hysteresis, defined as the difference between the advancing (sessile drop) and receding (captive bubble) contact angle, was also investigated. Specifically, the hysteresis of the pristine and HA-grafted pHEMA-co-TRIS materials was 55.0 ± 3.0° and 12.8 ± 3.6°, respectively. The significantly lower hysteresis (~80%) of the surface-modified model SiHy suggests lower surface heterogeneity and roughness because of the presence of the rigid hydrophilic layer of the grafted HA at the interface.[71,72] In CL applications,

the advancing contact angle and the hysteresis are suggested to be a good indication of clinically acceptable wettability and overall performance.[73] Reducing hysteresis is one of the ultimate goals in CL research and development.[6,71] These results are in agreement with those previously observed for the HA-grafted pHEMA materials, while also surface immobilization of HA-SH on vinyl- terminated glass surfaces via thiol-ene chemistry demonstrated improved surface wettability.[74]

Dehydration Profile and Swellability (EWC). CL dehydration, which occurs mainly due to environmental changes, may increase friction over time and thus can contribute to symptoms of ocular dryness and end-of-day discomfort.[75] Herein, the in vitro dehydration profile of the model SiHy was examined by calculating the rate of water evaporation (eq 2), using the gravimetric method. As shown in Figure 5, HA-grafted pHEMA-co-TRIS materials were characterized by a slower dehydration rate compared to the pristine and the intermediate samples. Moreover, the procedure of grafting HA to the surface of the pHEMA-co- TRIS SiHy was not found to alter the swellability of the materials, as the EWC of the unmodified pHEMA-co-TRIS (29.3 ± 0.8%) was not statistically different from that of the surface acrylated (27.9 ± 1.0%) and HA-grafted (29.2 ± 0.7%) SiHy samples ($p = 0.9$). These results are in accordance with previously published results for CL materials with HA on the surface.[40,50] Hence, the water binding properties of the surface- grafted HA layer not only enhanced the surface wettability of the model SiHy but also provided surfaces with improved water-retentive properties.

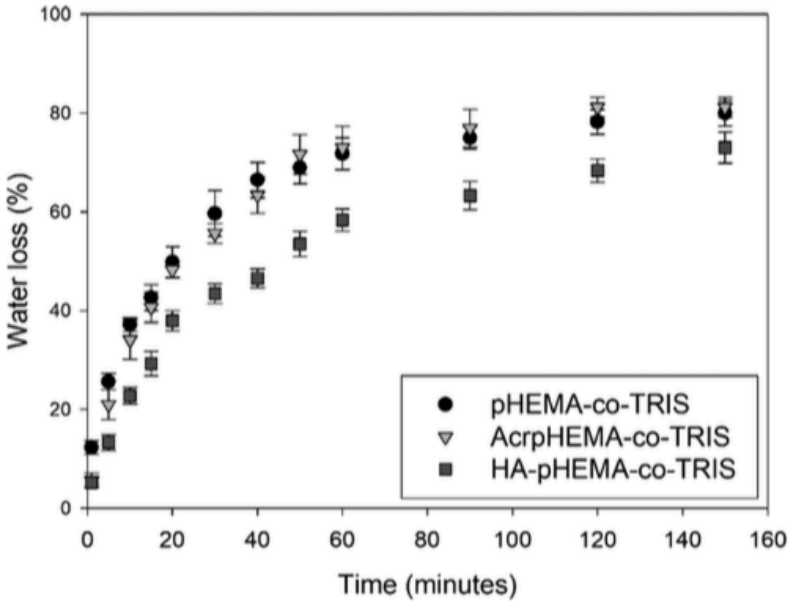


**Figure 5.** Dehydration profile expressed as the water loss (%) (±SD) over time from the pristine pHEMA-*co*-TRIS, Acr pHEMA-*co*-TRIS, and HA-pHEMA-*co*-TRIS SiHy in a controlled closed chamber ($T$ = 23 °C, RH = 32%) ($n$ = 6).

Optical Transmittance. The impact of the surface modification process on the optical properties of the HA- grafted pHEMA-co-TRIS SiHy is depicted in Figure 6.

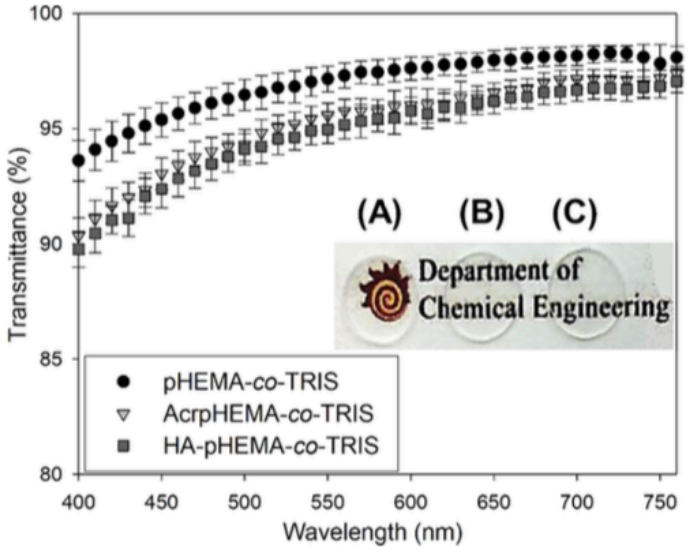


**Figure 6.** Transmittance spectra (±SD) and a photograph of the (A) pristine pHEMA-*co*-TRIS, (B) AcrpHEMA-*co*-TRIS, and (C) HA-pHEMA-*co*-TRIS discs ($n = 6$).

According to the results, the intermediate step of surface acrylation was found to cause a slight decrease (2%, $p < 0.0001$) in the measured transmittance. The immobilization reaction of HA on the surface of the pHEMA-co-TRIS materials was not found to further impact the optical acuity of the model SiHy with the transparency of these being above the acceptable range for CL applications (>90%). In addition, it is important to note that these materials have a thickness approximately 5 times higher than that of commercial CLs; hence, the suggested photochemical surface functionalization process described in this work is not expected to affect the optical performance of SiHy CLs.

Protein Deposition. The interactions of the CL surface with the proteins of the tear film play an important role in the compatibility of the lens with the ocular environment. Lysozyme (MW 14 kDa, pI 11) and HSA (MW 66 kDa, pI 4.7) were chosen as model proteins because they are among the major proteins found on worn SiHy CLs, and they are also associated with adverse effects.[14] Figure 7 shows the surface density of lysozyme and HSA on the pHEMA-co-TRIS materials. Surface acrylation of pHEMA-co-TRIS was found to increase the amount of lysozyme (20%, $p < 0.03$), whereas no statistical changes were observed for HSA ($p = 0.2$). Contrarily, the amount of lysozyme and HSA deposited on the HA-grafted pHEMA-co-TRIS was decreased by 30% ($p < 0.002$) and 45% ($p < 0.0004$), respectively, when compared to the pristine SiHy materials.

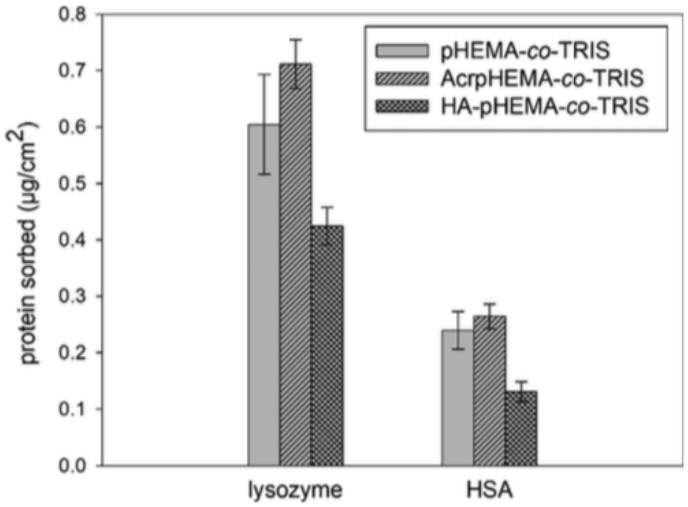


**Figure 7.** Amount (±SD) of lysozyme and HSA deposited in vitro on the surface of pristine pHEMA-*co*-TRIS, AcrpHEMA-*co*-TRIS, and HA-pHEMA-*co*-TRIS discs ($n$ = 6) upon a 6 h incubation period at room temperature.

The amount of lysozyme and HSA present on the pHEMA- co-TRIS surfaces was determined by protein radiolabeling, as this technique does not affect the absorption profile of the examined protein[76,77] and allows for the direct quantification of low amounts of adhered proteins with no need for prior chemical extraction.[78] According to the results, surface- immobilized HA on the surface of model SiHy via thiol- acrylate chemistry was able to retain its known antifouling properties, and thus its bioactivity, rendering it a good candidate for effective CL coating. The low-protein deposition could be further supported by the improved wettability, as shown by the reduced contact angles, exhibited by the HA- grafted pHEMA-co-TRIS surfaces since improving the surface hydrophilicity of biomaterials has been shown in general to reduce nonspecific protein deposition.[79–82] Consequently, the surface-grafted layer of the hydrophilic HA was speculated to suppress the thermodynamically unfavorable hydrophobic interactions between the proteins and the pHEMA-co-TRIS substrate, and thus, steric repulsion in combination with the hydration layer associated with the HA was considered as the primary contributors to the antifouling properties of the HA- modified SiHy surfaces. Parameters, including surface density, chain mobility, and conformational freedom of the surface- grafted HA layer, play key roles in the observed low-fouling properties herein.[62,83,84]

In addition, the surface density of lysozyme was consistently higher than the surface density of HSA (~65%, $p < 0.0001$) on all samples. This was likely due to the differences in MW, conformational stability, and net charge of the two proteins, as these parameters were previously found to contribute to the protein deposition profile.[38] When compared to

surface- modified HA-grafted pHEMA hydrogels,[50] the amount of lysozyme and HSA deposited on the these SiHy materials was lower. SiHy materials are known to attract less proteins than conventional hydrogel CLs. Future studies should also be considered to assess the antifouling properties of the HA- grafted pHEMA-co-TRIS surfaces upon incubation in multi- protein solution (artificial tear solution) because of the competitive sorption mechanism (Vroman effect).

In Vitro Cytotoxicity Study. The cytocompatibility of pHEMA-co-TRIS after each modification step is shown in Figure 8. The relative cell viability of all the three SiHy samples was almost 100%, indicating that the HA-grafted model SiHy showed little or no cytotoxicity. These results also suggest that the washing steps used during the surface modification procedure were appropriate for the removal of any leachable components that could cause toxic effects to the HCECs. Cytocompatible doses of I2959 were used in this work for the surface modification reaction, as previous studies showed that the viability of living cells was not affected when this concentration of I2959 was used for cell encapsulation polymerization reactions.[58] Additionally, immortalized HCECs are a well-established tool for screening in vitro ocular toxicity,[85] whereas MTT assay allows for reproducible toxicity testing.[86] Hence, the HA-grafting procedure used in this study has good potential for the modification of lens materials to improve surface properties.

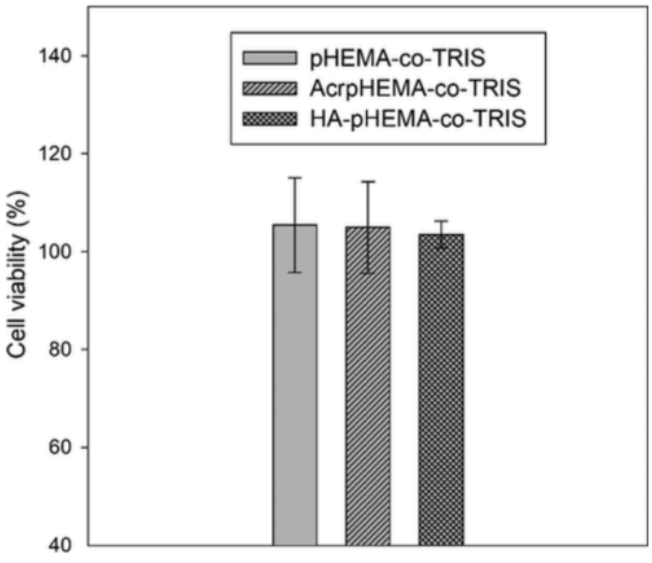


**Figure 8.** Cell viability (%) (±SD) of HCECs upon incubation with pristine pHEMA-*co*-TRIS, AcrpHEMA-*co*-TRIS, and HA-pHEMA-*co*-TRIS discs for 24 h ($n$ = 4) via MTT assay. Results expressed in respect to positive control (cell-only).

## CONCLUSIONS

In this work, HA was successfully grafted on the surface of model pHEMA-co-TRIS SiHy by UV-induced thiol-ene “click” chemistry, a versatile technique for tailored

surface properties. The intermediate surface acrylation and the presence of the surface-bound HA were confirmed by FTIR–ATR and XPS. The results indicated that grafting HA to the surface of the model pHEMA-co-TRIS SiHy improved the surface wettability, dehydration profile, and antifouling properties. In addition, the HA-grafted pHEMA-co-TRIS remained optically transparent and showed good in vitro compatibility with HCECs. Therefore, chemical immobilization of HA on the surface of SiHy may offer a promising means of coupling the advantageous bulk properties of SiHy with well-controlled interfacial properties, rendering these materials attractive candidates for biomaterial applications and more specifically as CLs. Future work will investigate the impact of the surface modification step with HA on the friction coefficient of the developed materials, as friction is considered an important parameter for on-eye comfort during CL wear.

## AUTHOR INFORMATION

Corresponding Author

*E-mail: sheardow@mcmaster.ca.

Notes

The authors declare no competing financial interests.

## ACKNOWLEDGEMENTS

This work was financially supported by Natural Sciences and Engineering Research Council (NSERC) of Canada and the 20/20 NSERC Ophthalmic Materials Research Network and is gratefully acknowledged. The authors would also like to thank Dr. Danielle Covelli (Biointerfaces Institute, McMaster University) for her help acquiring the AR-XPS spectra and Dr. Megan Dodd for her help with the cytotoxicity assay.

## REFERENCES

(1) Jones, L. Modern Contact Lens Materials: A Clinical Performance Update. Contact Lens Spectr. 2002, 17, 24–35.

(2) Sweeney, D. F. Clinical Performance of Silicone Hydrogel Lenses. In Silicone hydrogels: Continuous wear Contact Lenses; Butterworth-Heinemann: Oxford, 2004; pp 164–216.

(3)Compañ,V.;Andrio,A.;Loṕez-Alemany,A.;Riande,E.;Refojo, M. F. Oxygen Permeability of Hydrogel Contact Lenses with Organosilicon Moieties. Biomaterials 2002, 23, 2767–2772.

(4) Covey, M.; Sweeney, D. F.; Terry, R.; Sankaridurg, P. R.; Holden, B. A. Hypoxic Effects on the Anterior Eye of High-Dk Soft Contact Lens Wearers Are Negligible. Optom. Vis. Sci. 2001,

78, 95– 99.

(5) Bruinsma, G. M.; van der Mei, H. C.; Busscher, H. J. Bacterial Adhesion to Surface Hydrophilic and Hydrophobic Contact Lenses. Biomaterials 2001, 22, 3217–3224.

(6) Cheng, L.; Muller, S. J.; Radke, C. J. Wettability of Silicone- Hydrogel Contact Lenses in the Presence of Tear-Film Components. Curr. Eye Res. 2004, 28, 93–108.

(7) Tighe, B. Silicone Hydrogels: Structure, Properties and Behaviour. In Silicone Hydrogels: Continuous Wear Contact Lenses; Sweeney, D., Ed.; Butterworth-Heinemann: Oxford, 2004; pp 1–27.

(8)Lopez-Alemany,A.;Compañ,V.;Refojo,M.F.Porousstructure of Purevision versus Focus Night&Day and conventional hydrogel contact lenses. J. Biomed. Mater. Res. 2002, 63, 319–325.

(9) Jones, L.; Subbaraman, L.; Rogers, R.; Dumbleton, K. Surface Treatment, Wetting and Modulus of Silicone Hydrogels. Optician 2006, 232, 28–34.

(10) Steffen, R.; Schnider, C. A next Generation Silicone Hydrogel Lens for Daily Wear. Part 1 - Material Properties. Optician 2004, 227, 23–25.

(11) Jones, L.; Comfilcon, A. A New Silicone Hydrogel. Contact Lens Spectr. 2007, 22, 21.

(12) Stone, R. Introducing Water Gradient Technology. Contact Lens Spectr. 2013, 28, 34–38.

(13) Nichols, J. J. Continuing Upward Trends in Daily Disposable Prescribing and Other Key Segments Maintained a Healthy Industry. Contact Lens Spectr. 2018, 33, 42.

(14) Luensmann, D.; Jones, L. Protein Deposition on Contact Lenses: The Past, the Present, and the Future. Contact Lens Anterior Eye 2012, 35, 53–64.

(15) Panaser, A.; Tighe, B. J. J. Function of Lipids – Their Fate in Contact Lens Wear: An Interpretive Review. Contact Lens Anterior Eye 2012, 35, 100–111.

(16) Stapleton, F.; Keay, L.; Edwards, K.; Holden, B. The Epidemiology of Microbial Keratitis with Silicone Hydrogel Contact Lenses. Eye Contact Lens 2013, 39, 78–84.

(17) Richdale, K.; Sinnott, L. T.; Skadahl, E.; Nichols, J. J. Frequency of and Factors Associated With Contact Lens Dissat- isfaction and Discontinuation. Cornea 2007, 26, 168–174.

(18) Dumbleton, K.; Woods, C. A.; Jones, L. W.; Fonn, D. The Impact of Contemporary Contact Lenses on Contact Lens Discontinuation. Eye Contact Lens 2013, 39, 93–99.

(19) Jacob, J. T. Biocompatibility in the Development of Silicone- Hydrogel Lenses. Eye Contact Lens 2013, 39, 13–19.

(20)Jones,L.;Brennan,N.A.;Gonzaĺez-Meíjome,J.;Lally,J.; Maldonado-Codina, C.; Schmidt, T.

A.; Subbaraman, L.; Young, G.; Nichols, J. J. The TFOS International Workshop on Contact Lens Discomfort: Report of the Contact Lens Materials, Design, and Care Subcommittee. Invest. Ophthalmol. Vis. Sci. 2013, 54, TFOS37– TFOS70.

(21) Thissen, H.; Gengenbach, T.; du Toit, R.; Sweeney, D. F.; Kingshott, P.; Griesser, H. J.; Meagher, L. Clinical Observations of Biofouling on PEO Coated Silicone Hydrogel Contact Lenses. Biomaterials 2010, 31, 5510–5519.

(22) Wang, J. J.; Liu, F. Imparting Antifouling Properties of Silicone Hydrogels by Grafting Poly(Ethylene Glycol) Methyl Ether Acrylate Initiated by UV Light. J. Appl. Polym. Sci. 2012, 125, 548–554.

(23) Sun, F.-q.; Li, X.-s.; Cao, P.-t.; Xu, J.-k. Enhancing Hydrophilicity and Protein Resistance of Silicone Hydrogels by Plasma Induced Grafting with Hydrophilic Polymers. Chin. J. Polym. Sci. 2010, 28, 547–554.

(24) Goda, T.; Ishihara, K. Soft Contact Lens Biomaterials from Bioinspired Phospholipid Polymers. Expert Rev. Med. Devices 2006, 3, 167–174.

(25) Xu, C.; He, R.; Xie, B.; Ismail, M.; Yao, C.; Luan, J.; Li, X. Silicone Hydrogels Grafted with Natural Amino Acids for Ophthalmological Application. J. Biomater. Sci. Polym. Ed. 2016, 27, 1354–1368.

(26) Balazs, E. A.; Armand, G. Glycosaminoglycans and Proteoglycans of Ocular Tissues. Glycosaminoglycans and Proteoglycans in Physiological and Pathological Processes of Body Systems; S. Karger AG: Basel, 1982; pp 480–499.

(27) Yoshida, K.; Nitatori, T.; Uchiyama, Y. Localization of Glycosaminoglycans and CD44 in the Human Lacrimal Gland. Arch. Histol. Cytol. 1996, 59, 505–513.

(28) Lerner, L. E.; Schwartz, D. M.; Hwang, D. G.; Howes, E. L.; Stern, R. Hyaluronan and CD44 in the Human Cornea and Limbal Conjunctiva. Exp. Eye Res. 1998, 67, 481–484.

(29) Fukuda, K.; Miyamoto, Y. Hyaluronic Acid in Tear Fluid and Its Synthesis by Corneal Epithelial Cells. Asia-Pac. J. Ophthalmol. 1998, 40, 62–65.

(30)Kogan,G.;Šolteś,L.;Stern,R.;Gemeiner,P.HyaluronicAcid: A Natural Biopolymer with a Broad Range of Biomedical and Industrial Applications. Biotechnol. Lett. 2007, 29, 17–25.

(31) Fraser, J. R. E.; Laurent, T. C.; Laurent, U. B. G. Hyaluronan: Its Nature, Distribution, Functions and Turnover. J. Intern. Med. 1997, 242, 27–33.

(32) Hamano, T.; Horimoto, K.; Lee, M.; Komemushi, S. Sodium Hyaluronate Eyedrops Enhance Tear Film Stability. Jpn. J. Ophthalmol. 1996, 40, 62.

(33) Acosta, M. C.; Gallar, J.; Belmonte, C. The Influence of Eye Solutions on Blinking and Ocular Comfort at Rest and during Work at Video Display Terminals. Exp. Eye Res. 1999, 68, 663–669.

(34) O'Brien, P. D.; Collum, L. M. T. Dry Eye: Diagnosis and Current Treatment Strategies. Curr. Allergy Asthma Rep. 2004, 4, 314–319.

(35) Gonzaĺez-Meíjome, J. M.; da Silva, A. C.; Neves, H.; Lopes-Ferreira,D.;Queiroś,A.;Jorge,J.ClinicalPerformanceand"ExVivo" Dehydration of Silicone Hydrogel Contact Lenses with Two New Multipurpose Solutions. Contact Lens Anterior Eye 2013, 36, 86–92.

(36) Weeks, A.; Morrison, D.; Alauzun, J. G.; Brook, M. A.; Jones, L.; Sheardown, H. Photocrosslinkable Hyaluronic Acid as an Internal Wetting Agent in Model Conventional and Silicone Hydrogel Contact Lenses. J. Biomed. Mater. Res., Part A 2012, 100, 1972–1982.

(37) Weeks, A.; Subbaraman, L. N.; Jones, L.; Sheardown, H. Physical Entrapment of Hyaluronic Acid during Synthesis Results in Extended Release from Model Hydrogel and Silicone Hydrogel Contact Lens Materials. Eye Contact Lens 2013, 39, 179–185.

(38) Jeong, K.-S.; Kim, H.-J.; Lim, H.-L.; Ryu, G.-C.; Seo, E.-S.; You, N.-H.; Jun, J. Synthesis and Biocompatibility of Silicone Hydrogel Functionalized with Polysaccharide. Bull. Korean Chem. Soc. 2015, 36, 1649–1653.

(39)Weeks,A.;Boone,A.;Luensmann,D.;Jones,L.;Sheardown, H. The Effects of Hyaluronic Acid Incorporated as a Wetting Agent on Lysozyme Denaturation in Model Contact Lens Materials. J. Biomater. Appl. 2013, 28, 323–333.

(40) Singh, A.; Li, P.; Beachley, V.; McDonnell, P.; Elisseeff, J. H. A Hyaluronic Acid-Binding Contact Lens with Enhanced Water Retention. Contact Lens Anterior Eye 2015, 38, 79–84.

(41) Lin, C.-H.; Cho, H.-L.; Yeh, Y.-H.; Yang, M.-C. Improvement of the Surface Wettability of Silicone Hydrogel Contact Lenses via Layer-by-Layer Self-Assembly Technique. Colloids Surf., B 2015, 136, 735–743.

(42) Cassinelli, C.; Morra, M.; Pavesio, A.; Renier, D. Evaluation of Interfacial Properties of Hyaluronan Coated Poly- (Methylmethacrylate) Intraocular Lenses. J. Biomater. Sci. Polym. Ed. 2000, 11, 961–977.

(43) Guan, B.; Wang, H.; Xu, R.; Zheng, G.; Yang, J.; Liu, Z.; Cao, M.; Wu, M.; Song, J.; Li, N.; et al. Establishing Antibacterial Multilayer Films on the Surface of Direct Metal Laser Sintered Titanium Primed with Phase-Transited Lysozyme. Sci. Rep. 2016, 6, 36408.

(44) Morra, M. Engineering of Biomaterials Surfaces by Hyaluronan. Biomacromolecules 2005, 6, 1205–1223.

(45) Hoyle, C. E.; Bowman, C. N. Thiol-Ene Click Chemistry. Angew. Chem. Int. Ed. 2010, 49, 1540–1573.

(46) Nimmo, C. M.; Shoichet, M. S. Regenerative Biomaterials That "Click": Simple, Aqueous-Based Protocols for Hydrogel Synthesis, Surface Immobilization, and 3D Patterning. Bioconjug. Chem. 2011, 22, 2199–2209.

(47) Manhart, J.; Kramer, R.; Schaller, R.; Holzner, A.; Kern, W.; Schlögl, S. Surface Functionalization of Natural Rubber by UV- Induced Thiol-Ene Chemistry. Macromol. Symp. 2016, 365, 32–39.

(48) Iwasaki, Y.; Matsuno, H. Metabolic Delivery of Methacryloyl Groups on Living Cells and Cell Surface Modification via Thiol-Ene "Click" Reaction. Macromol. Biosci. 2011, 11, 1478–1483.

(49)Köwitsch,A.;Yang,Y.;Ma,N.;Kuntsche,J.;Mad¨er,K.;Groth, T. Bioactivity of Immobilized Hyaluronic Acid Derivatives Regarding Protein Adsorption and Cell Adhesion. Biotechnol. Appl. Biochem. 2011, 58, 376–389.

(50) Korogiannaki, M.; Zhang, J.; Sheardown, H. Surface Modification of Model Hydrogel Contact Lenses with Hyaluronic Acid via Thiol-Ene "Click" Chemistry for Enhancing Surface Characteristics. J. Biomater. Appl. 2017, 32, 446–462.

(51) Lowe, A. B. Thiol-Ene "Click" Reactions and Recent Applications in Polymer and Materials Synthesis. Polym. Chem. 2010, 1, 17–36.

(52) Wang, H.; Sun, H.; Wei, H.; Xi, P.; Nie, S.; Ren, Q. Biocompatible Hyaluronic Acid Polymer-Coated Quantum Dots for CD44+ Cancer Cell-Targeted Imaging. J. Nanoparticle Res. 2014, 16, 2621.

(53) Huo, Y.; Ketelson, H.; Perry, S. S. Ethylene Oxide-Block- Butylene Oxide Copolymer Uptake by Silicone Hydrogel Contact Lens Materials. Appl. Surf. Sci. 2013, 273, 472–477.

(54) Cumpson, P. J. Angle-Resolved XPS and AES: Depth- Resolution Limits and a General Comparison of Properties of Depth-Profile Reconstruction Methods. J. Electron Spectrosc. Relat. Phenom. 1995, 73, 25–52.

(55) McFarlane, A. S. Efficient Trace-Labelling of Proteins with Iodine. Nature 1958, 182, 53.

(56) Favuzza, E.; Mencucci, R.; Paladini, I.; Pellegrini-Giampietro, D. E.; Menchini, U.; Scartabelli, T. Azithromycin: Assessment of Intrinsic Cytotoxic Effects on Corneal Epithelial Cell Cultures. Clin. Ophthalmol. 2013, 7, 965–971.

(57) Getz, E. B.; Xiao, M.; Chakrabarty, T.; Cooke, R.; Selvin, P. R. A Comparison between the Sulfhydryl Reductants Tris(2- Carboxyethyl)Phosphine and Dithiothreitol for Use in Protein Biochemistry. Anal. Biochem. 1999, 273, 73–80.

(58) Bryant, S. J.; Nuttelman, C. R.; Anseth, K. S. Cytocompatibility of UV and Visible Light Photoinitiating Systems on Cultured NIH/ 3T3 Fibroblasts in Vitro. J. Biomater. Sci. Polym. Ed. 2000, 11, 439– 457.

(59) Hoyle, C. E.; Lowe, A. B.; Bowman, C. N. Thiol-Click Chemistry: A Multifaceted Toolbox for Small Molecule and Polymer Synthesis. Chem. Soc. Rev. 2010, 39, 1355–1387.

(60) Cramer, N. B.; Bowman, C. N. Kinetics of Thiol-Ene and Thiol-Acrylate

Photopolymerizations with Real-Time Fourier Trans- form Infrared. J. Polym. Sci., Part A: Polym. Chem. 2001, 39, 3311– 3319.

(61) Stile, R. A.; Barber, T. A.; Castner, D. G.; Healy, K. E. Sequential Robust Design Methodology and X-Ray Photoelectron Spectroscopy to Analyze the Grafting of Hyaluronic Acid to Glass Substrates. J. Biomed. Mater. Res. 2002, 61, 391–398.

(62) Morra, M.; Cassineli, C. Non-Fouling Properties of Polysaccharide-Coated Surfaces. J. Biomater. Sci. Polym. Ed. 1999, 10, 1107–1124.

(63) Hajati, S.; Tougaard, S. XPS for Non-Destructive Depth Profiling and 3D Imaging of Surface Nanostructures. Anal. Bioanal. Chem. 2010, 396, 2741–2755.

(64) Ton-That, C.; Shard, A. G.; Bradley, R. H. Thickness of Spin- Cast Polymer Thin Films Determined by Angle-Resolved XPS and AFM Tip-Scratch Methods. Langmuir 2000, 16, 2281–2284.

(65) Karlgard, C. C. S.; Sarkar, D. K.; Jones, L. W.; Moresoli, C.; Leung, K. T. Drying methods for XPS analysis of PureVision?, FocusS Night&Day? and conventional hydrogel contact lenses. Appl. Surf. Sci. 2004, 230, 106–114.

(66) Tighe, B. J. A Decade of Silicone Hydrogel Development: Surface Properties, Mechanical Properties, and Ocular Compatibility. Eye Contact Lens 2013, 39, 4–12.

(67) Mikhail, A. S.; Ranger, J. J.; Liu, L.; Longenecker, R.; Thompson, D. B.; Sheardown, H. D.; Brook, M. A. Rapid and Efficient Assembly of Functional Silicone Surfaces Protected by PEG: Cell Adhesion to Peptide-Modified PDMS. J. Biomater. Sci. Polym. Ed. 2010, 21, 821–842.

(68)Maldonado-Codina,C.;Morgan,P.B.Invitrowaterwettability of silicone hydrogel contact lenses determined using the sessile drop and captive bubble techniques. J. Biomed. Mater. Res., Part A 2007, 83, 496–502.

(69) Keir, N.; Jones, L. Wettability and Silicone Hydrogel Lenses: A Review. Eye Contact Lens 2013, 39, 100–108.

(70) Thai, L. C.; Tomlinson, A.; Ridder, W. H. Contact Lens Drying and Visual Performance: The Vision Cycle with Contact Lenses. Optom. Vis. Sci. 2002, 79, 381–388.

(71) Tonge, S.; Jones, L.; Goodall, S.; Tighe, B. The Ex Vivo Wettability of Soft Contact Lenses. Curr. Eye Res. 2001, 23, 51–59. (72) Tretinnikov, O. N.; Ikada, Y. Dynamic Wetting and Contact

Angle Hysteresis of Polymer Surfaces Studied with the Modified Wilhelmy Balance Method. Langmuir 1994, 10, 1606–1614.

(73) Read, M. L.; Morgan, P. B.; Kelly, J. M.; Maldonado-Codina, C. Dynamic Contact Angle Analysis of Silicone Hydrogel Contact Lenses. J. Biomater. Appl. 2011, 26, 85–99.

(74) Köwitsch, A.; Abreu, M. J.; Chhalotre, A.; Hielscher, M.; Fischer, S.; Mäder, K.; Groth, T. Synthesis of Thiolated Glycosaminoglycans and Grafting to Solid Surfaces. Carbohydr. Polym. 2014, 114, 344–351.

(75) Tighe, B. Silicone Hydrogel Materials How Do They Work? In Silicone Hydrogels: The Rebirth of Continuous Wear Contact Lenses; Sweeney, D. F., Ed.; Butterworth-Heinemann: Oxford, 2000; pp 1– 21.

(76) Regoeczi, E. Iodine-Labeled Plasma Proteins Vol. 1; CRC Press: Boca Raton, FL, 1984; Vol. 17.

(77) Carney, F. P.; Morris, C. A.; Milthorpe, B.; Flanagan, J. L.; Willcox, M. D. P. In Vitro Adsorption of Tear Proteins to Hydroxyethyl Methacrylate-Based Contact Lens Materials. Eye Contact Lens 2009, 35, 320–328.

(78) Hall, B.; Jones, L. W.; Forrest, J. A. Competitive Effects from an Artificial Tear Solution to Protein Adsorption. Optom. Vis. Sci. 2015, 92, 781–789.

(79) Willis, S. L.; Court, J. L.; Redman, R. P.; Wang, J.-H.; Leppard, S. W.; O'Byrne, V. J.; Small, S. A.; Lewis, A. L.; Jones, S. A.; Stratford, P. W. A Novel Phosphorylcholine-Coated Contact Lens for Extended Wear Use. Biomaterials 2001, 22, 3261–3272.

(80) Chen, H.; Brook, M. A.; Chen, Y.; Sheardown, H. Surface Properties of PEO-Silicone Composites: Reducing Protein Adsorp- tion. J. Biomater. Sci. Polym. Ed. 2005, 16, 531–548.

(81) Feng, W.; Brash, J.; Zhu, S. Non-Biofouling Materials Prepared by Atom Transfer Radical Polymerization Grafting of 2-Methacrylo- loxyethyl Phosphorylcholine: Separate Effects of Graft Density and Chain Length on Protein Repulsion. Biomaterials 2006, 27, 847–855.

(82) Andrade, J. D. Interfacial Phenomena and Biomaterials. Med. Instrum. 1973, 7, 110–120.

(83) Chen, S.; Li, L.; Zhao, C.; Zheng, J. Surface Hydration: Principles and Applications toward Low-Fouling/Nonfouling Bio- materials. Polymer 2010, 51, 5283–5293.

(84)Ademovic,´Z.;Maric,´S.;Kingshott,P.;Ilicǩovic,´Z.Hydrogels from Polyacrylic Acid for Reduction of Bioadhesion on Silicone Contact Lenses. Contemp. Mater. 2014, 1, 95–100.

(85) Huhtala, A.; Salminen, L.; Taḧti, H.; Uusitalo, H. Corneal Models for the Toxicity Testing of Drugs and Drug Releasing Materials. Topics in Multifunctional Biomaterials and Devices; University of Oulu, 2008; pp 1–24.

(86) Offord, E. A.; Sharif, N. A.; Mace,´ K.; Tromvoukis, Y.; Spillare, E. A.; Avanti, O.; Howe, W. E.; Pfeifer, A. M. Immortalized Human Corneal Epithelial Cells for Ocular Toxicity and Inflammation Studies. Invest. Ophthalmol. Vis. Sci. 1999, 40, 1091–1101.